Received: 6 October 2022 | Revised: 24 August 2023 | Accepted: 28 August 2023

DOI: 10.1002/pamm.202200102

PAMM Proceedings in Applied Mathematics and Mechanics

RESEARCH ARTICLE

Elliptic operators with discontinuous coefficients in meshfree GFDM

Heinrich Kraus[1,2] | **Jörg Kuhnert**[2] | **Andreas Meister**[1] | **Pratik Suchde**[2,3]

[1]Universität Kassel, Kassel, Germany

[2]Fraunhofer ITWM, Kaiserslautern, Germany

[3]University of Luxembourg, Esch-sur-Alzette, Luxembourg

Correspondence
Heinrich Kraus, Universität Kassel, Heinrich-Plett-Straße 40, 34132 Kassel, Germany.
Email: heinrich.kraus@itwm.fraunhofer.de

Abstract

In phase change simulations, material properties such as density, viscosity, or thermal conductivity may exhibit jump discontinuities, possibly of several orders of magnitude. These jump discontinuities represent interfaces between the phases, and they emerge naturally during the simulation; thus, their exact location is generally unknown a priori. Our goal is to simulate phase change processes with a meshfree generalized finite difference method in a monolithic model without distinguishing between the different phases. There, the material properties mentioned above appear as coefficients inside elliptic operators in divergence form and the jumps must be treated adequately by the numerical method. We present a numerical method for discretizing elliptic operators with discontinuous coefficients without the need for a domain decomposition or tracking of interfaces. Our method facilitates the construction of diagonally dominant diffusion operators that lead to M-matrices for the discrete Poisson's equation, and thus, satisfy the discrete maximum principle. We demonstrate the applicability of the new method for the case of smooth diffusivity and discontinuous diffusivity. We show that the method is first-order accurate for discontinuous diffusion problems and provides second-order and fourth-order convergence for continuous diffusion coefficients.

1 | MOTIVATION

Phase change simulations lead to discontinuous coefficients in diffusion operators of the form

$$\Delta_\eta u = \nabla \cdot (\eta \nabla u).$$

Such diffusion operators appear in both momentum and energy conservation equations, where η can be the viscosity, the heat conductivity, or density [1, 2]. Our goal is to find a discrete diffusion operator using a meshfree method. We will test the discrete diffusion operator by using Poisson's equation

$$-\nabla \cdot (\eta \nabla u) = f, \tag{1}$$

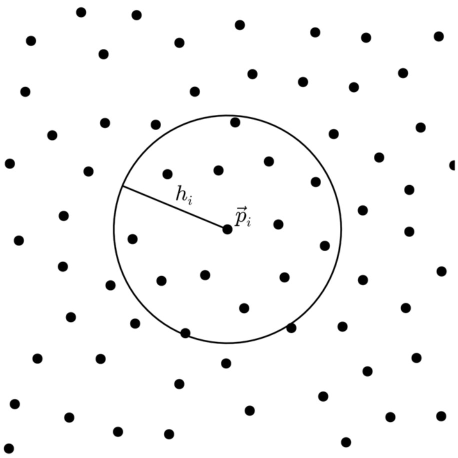

(A) Distance-based neighborhood S_i with radius h_i.

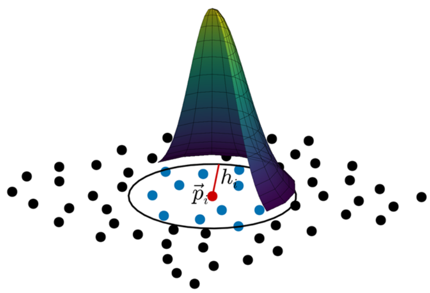

(B) Weighting kernel to define optimization problem.

FIGURE 1 Neighborhood S_i and weighting kernel.

on a domain Ω where f is a source function. Additionally, we set a Dirichlet boundary condition

$$u|_{\partial\Omega} = 0.$$

2 | GENERALIZED FINITE DIFFERENCE METHOD

The generalized finite difference method (GFDM) uses a point cloud

$$\Omega_h = \{\vec{p}_1, \dots, \vec{p}_N\} \subset \overline{\Omega} = \Omega \cup \partial\Omega,$$

to spatially discretize a domain $\Omega \subset \mathbb{R}^d$. We use the notation $u_i = u(\vec{p}_i)$ for evaluations of an arbitrary function $u : \Omega \to \mathbb{R}$. We restrict ourselves to the two-dimensional case $d = 2$ and use the notation

$$\vec{p}_i = \begin{pmatrix} x_i \\ y_i \end{pmatrix}.$$

To establish a notion of connectivity, we use a continuous function $h : \Omega \to (0, \infty)$ to establish neighborhoods as in Figure 1(A) of the form

$$S_i = \{ j : \|\vec{p}_j - \vec{p}_i\| < h_i \},$$

on which the discrete differential operators are defined. The function h also determines the refinement level of the point cloud, where an increasing refinement $h \to 0$ leads to an increasing number of points $N \to \infty$. The limit $h \to 0$ denotes that h converges uniformly to the zero function, and thus, the largest neighborhood radius $h_{\max} = \max_{i=1,\dots,N} h_i$ fulfills

$$h_{\max} \leq \|h\|_\infty \to 0,$$

as $h \to 0$ uniformly. In the examples presented below, we consider h to be a constant function, such that the resulting point clouds are "uniform" as in the cutout in Figure 1(A). In this case, the limit $h \to 0$ can be seen as the limit of a sequence of real numbers.

For a differential operator D^*, a discrete differential operator D_i^* is given by coefficients c_{ij}^* such that

$$D^* u(\vec{p}_i) \approx D_i^* u = \sum_{j \in S_i} c_{ij}^* u_j.$$

The asterisk is a placeholder for the differential operator that we want to discretize, for example, D^x and D^y are the directional derivatives in the x- and y-directions, respectively, and D^Δ is the Laplace operator.

There are numerous ways of determining the coefficients c^*_{ij}. One popular approach is by using a weighted least squares (WLSQ) optimization problem. For that, we assign a weight w_{ij} to each point $j \in S_i$ where further away points get a lower weight, see Figure 1(B) for an example. With these weights, we formulate a minimization problem

$$\min \sum_{j \in S_i} \left(\frac{c^*_{ij}}{w_{ij}} \right)^2, \tag{2a}$$

together with constraints

$$D^* \phi(\vec{p}_i) = \sum_{j \in S_i} c^*_{ij} \phi(\vec{p}_j), \tag{2b}$$

for test functions ϕ. The constraints enforce the discrete operator to be exact for specific test functions, and we usually use monomial test functions

$$\phi \in \{1, x - x_i, y - y_i, (x - x_i)^2, (x - x_i)(y - y_i), (y - y_i)^2, \dots\}.$$

For the discrete Laplace operator given by c^Δ_{ij}, it is also necessary to perform a one-dimensional correction technique to enforce diagonal dominance [3].

3 | DIFFUSION OPERATOR

To obtain the discrete diffusion operator $D_i^{\Delta_\eta}$, we present two approaches. One that is based on the WLSQ formulation and a novel formulation that scales the discrete Laplace operator.

To compute the WLSQ-based coefficients $c_{ij}^{\Delta_\eta}$, we need to ensure the exact reproducibility property for monomial test functions

$$\Delta_\eta 1|_{\vec{p}=\vec{p}_i} = 0, \tag{3a}$$

$$\Delta_\eta (x - x_i)|_{\vec{p}=\vec{p}_i} = \partial_x \eta(\vec{p}_i), \tag{3b}$$

$$\Delta_\eta (y - y_i)|_{\vec{p}=\vec{p}_i} = \partial_y \eta(\vec{p}_i), \tag{3c}$$

$$\Delta_\eta (x - x_i)^2|_{\vec{p}=\vec{p}_i} = 2\eta(\vec{p}_i), \tag{3d}$$

$$\Delta_\eta (x - x_i)(y - y_i)|_{\vec{p}=\vec{p}_i} = 0, \tag{3e}$$

$$\Delta_\eta (y - y_i)^2|_{\vec{p}=\vec{p}_i} = 2\eta(\vec{p}_i). \tag{3f}$$

We can see from the reproducibility conditions (3b) and (3c) that the gradient of η needs to be known or computed numerically. However, for a discontinuous diffusivity η, the strong-form gradient is undefined, and this method leads to high errors [2]. One reason for this behavior is the lack of diagonal dominance of the coefficients $c_{ij}^{\Delta_\eta}$ for η having discontinuities of several orders of magnitude.

To overcome these issues, we present a new way of defining a gradient-free discrete diffusion operator by using the coefficients

$$f_{ij}^{\Delta_\eta} = \eta_{ij} c^\Delta_{ij}, \tag{4a}$$

$$f_{ii}^{\Delta_\eta} = -\sum_{\substack{j \in S_i \\ j \neq i}} \eta_{ij} c^\Delta_{ij}, \tag{4b}$$

with reconstructions η_{ij} of η at the midpoint between $\vec{p}_i$ and $\vec{p}_j$

$$\eta_{ij} \approx \eta\left(\frac{\vec{p}_i + \vec{p}_j}{2}\right).$$

In our examples, we use the arithmetic average $\eta_{ij} = \frac{\eta_i + \eta_j}{2}$. It is easy to show that

$$\Delta_\eta u(\vec{p}_i) = \sum_{j \in S_i} f_{ij}^{\Delta_\eta} u_j + O(h_i^q + h_i^p),\ h \to 0,$$

holds, if the conditions

$$\Delta u(\vec{p}_i) = \sum_{j \in S_i} c_{ij}^{\Delta} u_j + O(h_i^p),\ h \to 0,$$

and

$$\eta_{ij} = \eta\left(\frac{\vec{p}_i + \vec{p}_j}{2}\right) + O(h_i^q),\ h \to 0,$$

are fulfilled. By using the notation $O(h_i^p)$, we emphasize that we fix the point $\vec{p}_i$ while refining the point cloud as $h \to 0$ uniformly. Thus, the coefficients $f_{ij}^{\Delta_\eta}$ provide a consistent discrete diffusion operator in the case of a smooth diffusivity η.

Discretizing Poisson's Equation (1) with the coefficients $f_{ij}^{\Delta_\eta}$, we obtain the linear system

$$\boldsymbol{D}^{\Delta_\eta} \boldsymbol{u} = \boldsymbol{f},$$

and if $f_{ij}^{\Delta_\eta}$ are diagonally dominant, then $\boldsymbol{D}^{\Delta_\eta}$ is an M-matrix [4]. If the coefficients c_{ij}^{Δ} are diagonally dominant, and the reconstructions η_{ij} are positive, then the coefficients $f_{ij}^{\Delta_\eta}$ are diagonally dominant as well, and we obtain a numerical scheme that satisfies the discrete maximum principle

$$\boldsymbol{f} \geq 0 \Rightarrow \boldsymbol{u} = (\boldsymbol{D}^{\Delta_\eta})^{-1} \boldsymbol{f} \geq 0.$$

In the case that the coefficients c_{ij}^{Δ} are not diagonally dominant, an alternative GFDM formulation that guarantees diagonal dominance may be used [2].

4 | NUMERICAL EXPERIMENTS

We provide two test cases to evaluate the discrete diffusion coefficients, one with a continuous diffusivity η and one with a discontinuous diffusivity. For sufficiently smooth functions $\overline{u}$ and η, we can define the source term by expanding the diffusion operator $f = -\nabla \cdot (\eta \nabla u) = -\nabla\eta \cdot \nabla\overline{u} - \eta\Delta\overline{u}$. If η is discontinuous along a level curve of $\overline{u}$ corresponding to a height $H > 0$ given by $\{\, \vec{p} \in \overline{\Omega} \mid \overline{u}(\vec{p}) = H \,\}$, then $u = (\overline{u} - H)/\eta + H$ is an analytic weak solution to Poisson's equation with the smooth source term $f = -\Delta\overline{u}$.

On a rectangular domain $\Omega = (-1, 1) \times (-1, 1)$, we use for both cases the base function $\overline{u}(\vec{p}) = \cos(\pi x/2)\cos(\pi y/2)$ (see Figure 3A) and the contour height $H = 3/4$. With this, we define the smooth diffusivity as $\eta_{\text{smooth}} = \tanh(4(\overline{u} - H)) + 2$, and the discontinuous diffusivity with a jump of eight orders of magnitude as

$$\eta_{\text{disc}}(\vec{p}) = \begin{cases} 10^8, & \text{if } \overline{u}(\vec{p}) \geq H, \\ 1, & \text{if } \overline{u}(\vec{p}) < H. \end{cases}$$

The diffusivities are shown in Figure 2. Homogeneous Dirichlet boundary conditions are set for both test cases, and we fix the right-hand side f as described above such that the respective solutions from Figure 3 are obtained.

For both test cases, we use the WLSQ approach by enforcing the consistency conditions (3) in the optimization problem (2). We compute the gradient of η numerically, using a second-order GFDM discrete gradient operator. We use consistency

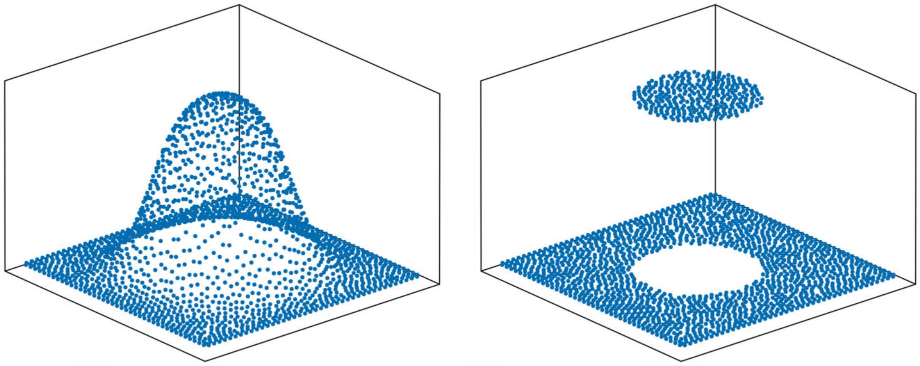

(A) Smooth diffusivity η_{smooth}.

(B) Discontinuous diffusivity η_{disc}.

FIGURE 2 Diffusivities η used in the two test cases considered for Poisson's Equation (1).

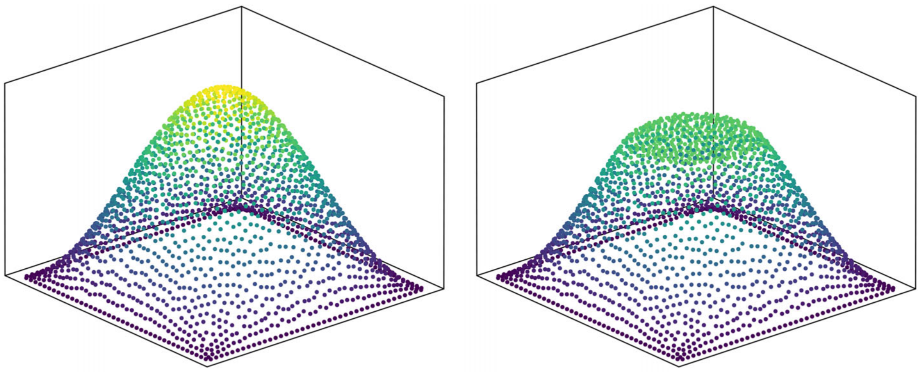

(A) Smooth

(B) Discontinuous

FIGURE 3 Analytical solution u to Poisson's equation with the respective diffusivities in Figure 2.

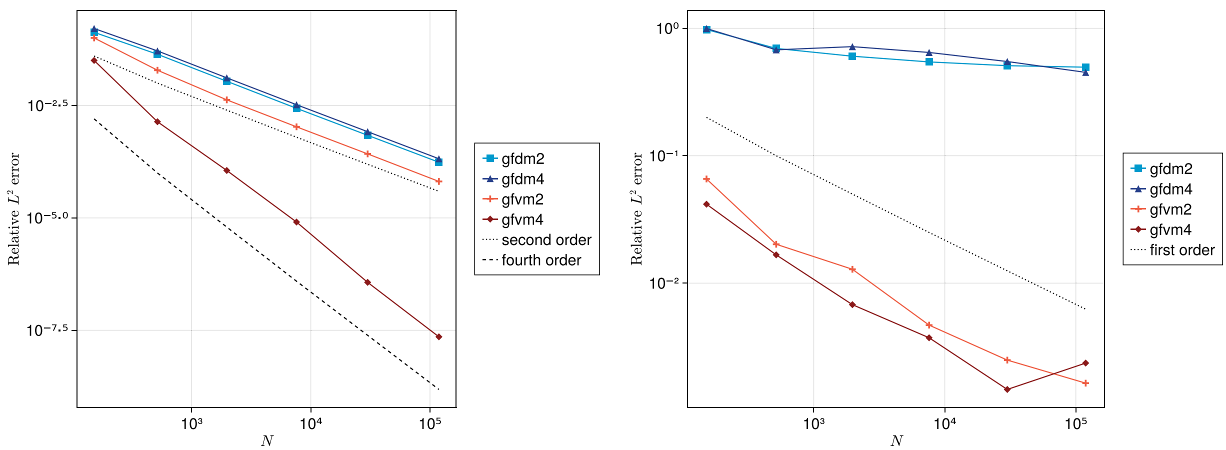

(A) Smooth diffusivity.

(B) Discontinuous diffusivity.

FIGURE 4 Errors depending on the number of points N.

conditions for monomials up to degree k and name the method gfdm$k$ in the figures below. The second method that uses the coefficients from Equation (4) is called gfvm$k$ if the underlying discrete Laplace operator, given by c^{Δ}_{ij}, is computed using consistency conditions for monomials up to degree k.

Let us first discuss the case of the smooth diffusivity, as shown in Figure 2(A) with its respective analytical solution in Figure 3(A). The results are shown in Figure 4(A). We observe that all methods are at least second-order accurate. We see that gfdm4 is only second-order accurate, and this is due to the numerical gradients being only second-order convergent. Furthermore, we find that gfvm4 shows fourth-order convergence.

Now, let us take a look at the case of a discontinuous diffusivity as shown in Figure 2(B) with a jump of eight orders of magnitude. The solution in Figure 3(B) exhibits a kink at the discontinuity of η. This test case poses great challenges to the numerical scheme, and generally, the strong-form GFDM does not provide satisfying results [2]. We can confirm this in our test case by looking at the error plots in Figure 4(B) where both gfdm2 and gfdm4 do not converge. However, both gfvm2 and gfvm4 show at least first-order convergence. Higher-order methods are possible by using aligned point clouds and setting interface conditions [5].

5 | CONCLUSION

We presented a novel formulation for the discrete diffusion operator. The new formulation does not depend on calculating the gradient of the diffusivity, and in our numerical experiments, it transfers the accuracy of the underlying discrete Laplace operator for continuous diffusion problems. For discontinuous diffusion problems, first-order convergence is achieved, which is expected for a method that uses nonaligned point clouds.

ACKNOWLEDGMENTS

Pratik Suchde would like to acknowledge support from the European Union's Horizon 2020 research and innovation program under the Marie Skłodowska-Curie Actions grant agreement No. 892761 "SURFING."

Open access funding enabled and organized by Projekt DEAL.

ORCID

Heinrich Kraus https://orcid.org/0000-0003-3984-9792

REFERENCES

1. Suchde, P., Kraus, H., Bock-Marbach, B., & Kuhnert, J. (2022). Meshfree one-fluid modelling of liquid-vapor phase transitions. Preprint arXiv:2203.10383.
2. Kraus, H., Kuhnert, J., Meister, A., & Suchde, P. (2023). A meshfree point collocation method for elliptic interface problems. *Applied Mathematical Modelling*, *113*, 241–261.
3. Suchde, P. (2018). *Conservation and accuracy in meshfree generalized finite difference methods* (PhD thesis). Technische Universität Kaiserslautern.
4. Seibold, B. (2006). *M-matrices in meshless finite difference methods* (PhD thesis). Technische Universität Kaiserslautern.
5. Davydov, O., & Safarpoor, M. (2021). A meshless finite difference method for elliptic interface problems based on pivoted QR decomposition. *Applied Numerical Mathematics*, *161*, 489–509.

How to cite this article: Kraus, H., Kuhnert, J., Meister, A., & Suchde, P. (2023). Elliptic operators with discontinuous coefficients in meshfree GFDM. *Proceedings in Applied Mathematics and Mechanics*, *23,* e202200102. https://doi.org/10.1002/pamm.202200102